0031-3998/01/5002-0172
PEDIATRIC RESEARCH

Vol. 50, No. 2, 2001
*Printed in U.S.A.*

# ARTICLES

# Gadolinium Chloride Inhibits Pulmonary Macrophage Influx and Prevents $O_2$-Induced Pulmonary Hypertension in the Neonatal Rat

ROBERT P. JANKOV, XIAOPING LUO, ROSETTA BELCASTRO, IAN COPLAND, HELENA FRNDOVA, STEPHEN J. LYE, JOHN R. HOIDAL, MARTIN POST, AND A. KEITH TANSWELL

*Canadian Institutes of Health Research Groups in Lung Development, Toronto, Ontario, Canada [R.P.J., X.L., R.B., H.F., I.C., M.P., A.K.T.]; Lung Biology Programme, Hospital for Sick Children Research Institute, and Developmental and Fetal Health, Samuel Lunenfeld Research Institute, Mt. Sinai Hospital, Toronto, Ontario, Canada [S.J.L.]; the Departments of Obstetrics and Gynaecology [S.J.L], Paediatrics [M.P., A.K.T] and Physiology [S.J.L., M.P., A.K.T.], University of Toronto, Toronto, Ontario, Canada; and the Department of Internal Medicine, University of Utah Health Sciences Center, Salt Lake City, Utah, U.S.A. [J.R.H.]*

## ABSTRACT

Newborn rats exposed to 60% $O_2$ for 14 d demonstrated a bronchopulmonary dysplasia-like lung morphology and pulmonary hypertension. A 21-aminosteroid antioxidant, U74389G, attenuated both pulmonary hypertension and macrophage accumulation in the $O_2$-exposed lungs. To determine whether macrophage accumulation played an essential role in the development of pulmonary hypertension in this model, pups were treated with gadolinium chloride ($GdCl_3$) to reduce lung macrophage content. Treatment of 60% $O_2$-exposed animals with $GdCl_3$ prevented right ventricular hypertrophy ($p < 0.05$) and smooth muscle hyperplasia around pulmonary vessels, but had no effect on morphologic changes in the lung parenchyma. In addition, $GdCl_3$ inhibited 60% $O_2$-mediated increases in endothelin-1, 8-isoprostane, and nitrotyrosine residues. Organotypic cultures of fetal rat distal lung cells were subjected to cyclical mechanical strain to assess the potential role of $GdCl_3$-induced blockade of stretch-mediated cation channels in these effects. Mechanical strain caused a moderate increase of endothelin-1 ($p < 0.05$), which was unaffected by $GdCl_3$, but had no effect on 8-isoprostane or nitric oxide synthesis. A critical role for endothelin-1 in $O_2$-mediated pulmonary hypertension was confirmed using the combined endothelin receptor antagonist SB217242. We concluded that pulmonary macrophage accumulation, in response to 60% $O_2$, mediated pulmonary hypertension through upregulation of endothelin-1. **(*Pediatr Res* 50: 172–183, 2001)**

**Abbreviations:**
**BPD,** bronchopulmonary dysplasia
**DMEM,** Dulbecco's modified Eagle's Medium
**ET-1,** endothelin-1
**FBS,** fetal bovine serum
**$GdCl_3$,** gadolinium chloride
**PDVF,** polyvinylidene difluoride
**ROS,** reactive oxygen species
**RVH,** right ventricular hypertrophy

Chronic neonatal lung injury, or BPD, remains an important cause of morbidity and mortality in preterm infants requiring respiratory support with mechanical ventilation and prolonged use of supplemental $O_2$ (1–3). Despite well-recognized changes in the usual histopathological features of BPD over the last three decades (4), infants with early respiratory failure (5) or established BPD (6) remain at increased risk of developing pulmonary hypertension, which is a recognized predictor of subsequent morbidity and mortality (7–9). Although the pathologic changes in the pulmonary vasculature of infants with severe BPD are well characterized (10, 11), the causes of aberrant pulmonary vascular development seen in BPD are

Received September 28, 2000; accepted March 20, 2001.
Correspondence: Dr. Keith Tanswell, Division of Neonatology, Hospital for Sick Children, 555 University Avenue, Toronto, Ontario M5G 1X8, Canada; e-mail: keitht@sickkids.on.ca
Supported, in part, by group grants from the Canadian Institutes of Health Research, and an equipment grant from the Ontario Thoracic Society. Dr. Tanswell holds the Women's Auxiliary Chair in Neonatal Medicine. Dr. Jankov is supported by a RESTRACOM Fellowship from the Hospital for Sick Children Research Institute.
R.P.J. and X.L. contributed equally to this work.

poorly understood. Current evidence implicates ROS, generated in excess of antioxidant defenses, in the pathogenesis of BPD (12). However, it is unclear whether ROS contribute specifically to the development of pulmonary hypertension.

Pulmonary macrophages are known to produce many vasoactive, mitogenic, and proinflammatory cytokines that have been implicated in tissue injury (13–15). The macrophage content in the lung is normally negligible *in utero*, though it increases slightly toward term with further increases in the early postnatal period (16). Interstitial and alveolar macrophages are seen in exaggerated numbers in preterm infants who are destined to develop BPD (17). They are also the predominant inflammatory cell type in infants with established BPD (18). Macrophages isolated from the airways of infants with BPD demonstrate an increase in ROS production relative to macrophages from infants without BPD (18).

Normal pulmonary arterial development in the postnatal rat lung is very similar to that seen in the human (19, 20), making the newborn rat a useful model for the study of pathologic changes in the pulmonary vasculature. We have described a newborn rat model with BPD-like histopathology (21) and pulmonary hypertension (22) induced by exposure to 60% $O_2$ for 14 d. Pathologic changes in the distal lung include both areas of parenchymal thickening and areas with an emphysema-like appearance. This appearance is consistent with failure of septation from inhibition of peripheral cell growth (21, 23), as described for human infants (4). Manifestations of pulmonary hypertension in this model, which include RVH and pulmonary arterial smooth muscle hyperplasia, were reversed by treatment with a 21-aminosteroid antioxidant, U74389G (24). The U74389G-mediated effect on pulmonary hypertension seemed to be secondary to inhibition of an 8-isoprostane-induced upregulation of ET-1 expression by 60% $O_2$ (24). As described below, we subsequently observed that 60% $O_2$-exposed animals treated with U74389G had an attenuated macrophage influx into the lung. This led us to hypothesize that vasoactive compounds such as ET-1 (14), derived directly or indirectly from alveolar macrophages, may play a causative role in the pulmonary vascular changes observed in this model. To test this hypothesis, we examined the modifying effect of $GdCl_3$ on lung macrophage content after

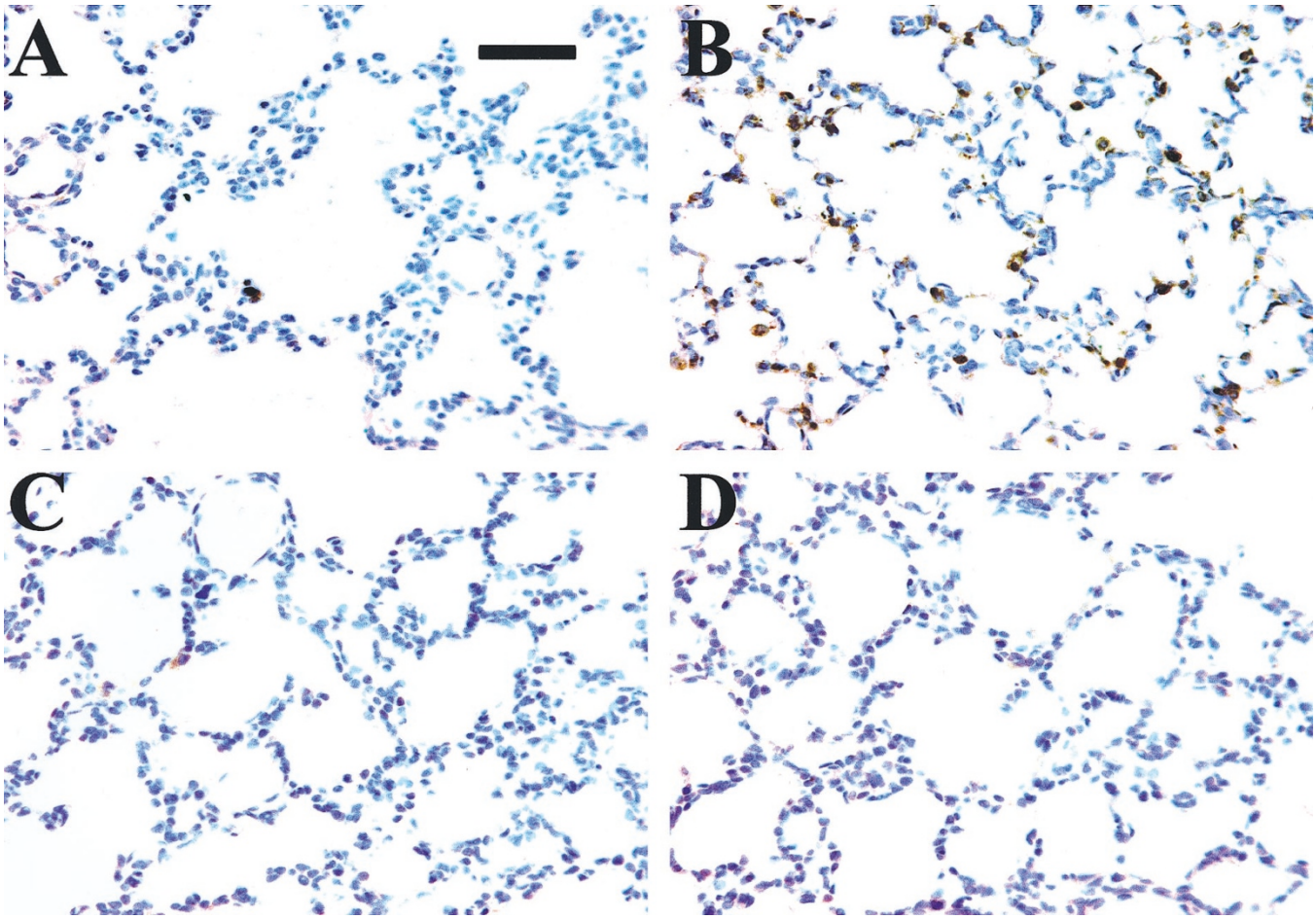


**Figure 1.** Lung macrophage content and the effect of treatment with U74389G. Immunohistochemistry for macrophage TPRM-2 antigen (*brown stain*) in lung tissue after exposure to air or 60% $O_2$ for 14 d. Newborn rats received daily i.p. injections of U74389G (10 mg/kg) in CS-4 vehicle or CS-4 vehicle alone. Bar length = 250 $\mu$m. (*A*) Interstitial macrophages were evident in air-exposed pups that received vehicle. (*B*) The macrophage content of the lungs of 60% $O_2$-exposed pups that received vehicle was markedly increased. (*C*) The lungs of air-exposed pups that received U74389G. (*D*) The 60% $O_2$-exposed pups that received U74389G had a similar macrophage content to air-exposed control animals.

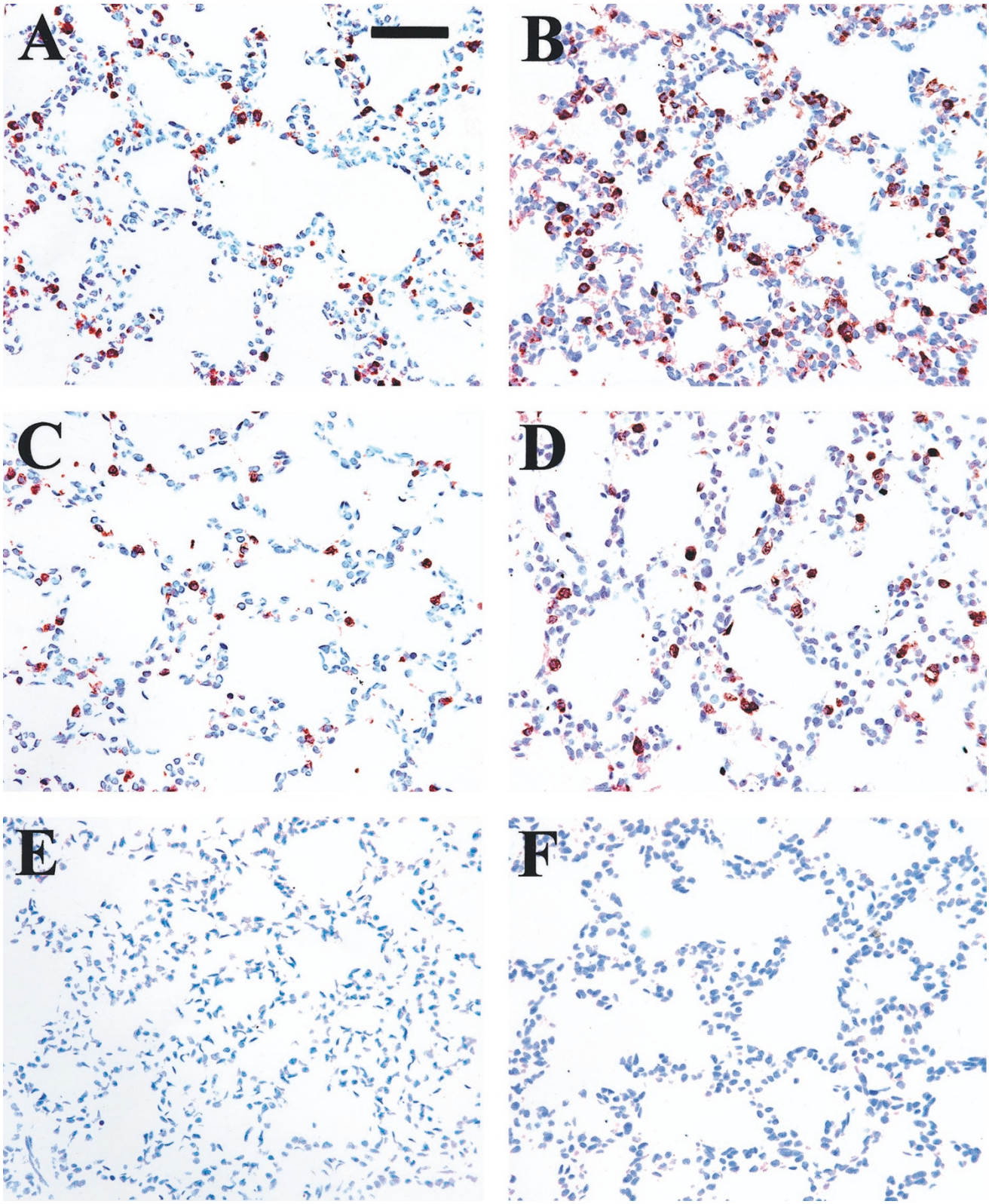


**Figure 2.** Lung macrophage content and the effect of treatment with $GdCl_3$. Immunohistochemistry for macrophage TPRM-2 cytoplasmic antigen (*brown stain*) in lung tissue after exposure to air or 60% $O_2$ for 7 d. Newborn rats received i.p. injections on d 0 and d 7 of $GdCl_3$ (10 mg/kg) in 0.9% saline vehicle or 0.9% saline vehicle alone. Bar length = 250 $\mu$m. (*A*) Interstitial macrophages were evident in air-exposed pups that received vehicle. (*B*) The macrophage content of the lungs of 60% $O_2$-exposed pups that received vehicle was markedly increased. (*C*) The lungs of air-exposed pups that received $GdCl_3$ had a slight reduction in macrophage content. (*D*) The 60% $O_2$-exposed pups that received $GdCl_3$ had a similar macrophage content to air-exposed control animals. (*E*) The lungs of pups on d 0, before $GdCl_3$ injection, had a negligible macrophage content. (*F*) Control slides, from which the primary antiserum was omitted, showed no staining.

exposure to 60% $O_2$. $GdCl_3$ is a rare earth lanthanide that has been used to abrogate macrophage migration and activation *in vivo* to delineate their role in disease. In animals, it has been reported to be effective in preventing pulmonary injury induced by ozone inhalation (25) and ovine lentivirus infection (26).

## METHODS

***Materials.*** $GdCl_3.6H_2O$ and BSA type V were from Sigma Chemical Co. (St. Louis, MO, U.S.A.). U74389G and CS-4 vehicle (20 mM citric acid monohydrate, 3.2 mM sodium citrate dihydrate, 77 mM NaCl, pH 3.0) were provided by Dr. D. Zimmerman (Pharmacia & Upjohn, Kalamazoo, MI, U.S.A.). SB217242 was kindly provided by Dr. Douglas Hay (SmithKline Beecham Pharmaceuticals, King of Prussia, PA, U.S.A.). Organic solvents were of HPLC grade. Peroxynitrite and a rabbit polyclonal antibody to nitrotyrosine were from Upstate Biotechnology (Lake Placid, NY, U.S.A.). Rabbit polyclonal antibody to human ET-1 was purchased from Chemicon (Temecula, CA, U.S.A.). Goat anti-rabbit IgG-peroxidase antibody was from Boehringer Mannheim (Mannheim, Germany) and goat anti-mouse IgG-peroxidase was from Calbiochem (La Jolla, CA, U.S.A). Goat anti-rabbit and goat anti-mouse IgG-biotin antibodies were from Santa Cruz Biotechnology (Santa Cruz, CA, U.S.A.). Mouse MAb to rat TPRM-2 macrophage protein, a cytoplasmic protein specific to rat macrophages, was obtained from BMA (Augst, Switzerland). Mouse MAb to $\alpha$-smooth muscle actin was from Neomarkers (Fremont, CA, U.S.A.). Avidin-biotin-peroxidase and alkaline phosphatase complex immunohistochemistry kits were purchased from Vector Laboratories (Burlingame, CA, U.S.A.). A total nitric oxide colorimetric assay kit was from R&D Systems (Minneapolis, MN, U.S.A.). ET-1 and 8-isoprostane enzyme immunoassay kits were from Cayman Chemical Co. (Ann Arbor, MI, U.S.A.), a total protein assay kit was from BioRad (Hercules, CA, U.S.A.), and Sep Pak C18 cartridges were from Waters (Mississauga, ON, Canada). [$^3$H]Prostaglandin $F_{2\alpha}$ was purchased from Dupont NEN Products (Boston, MA, U.S.A.). Gels and membranes were from Novex (San Diego, CA, U.S.A.). Cell culture media, antibiotics, and trypsin were from GIBCO (Burlington, ON, Canada). Gelfoam sponges were from Pharmacia & Upjohn (Toronto, ON, Canada). FBS was from Flow Laboratories (McLean, VA, U.S.A.), and collagenase and DNase were from Worthington (Freehold, NJ, U.S.A.).

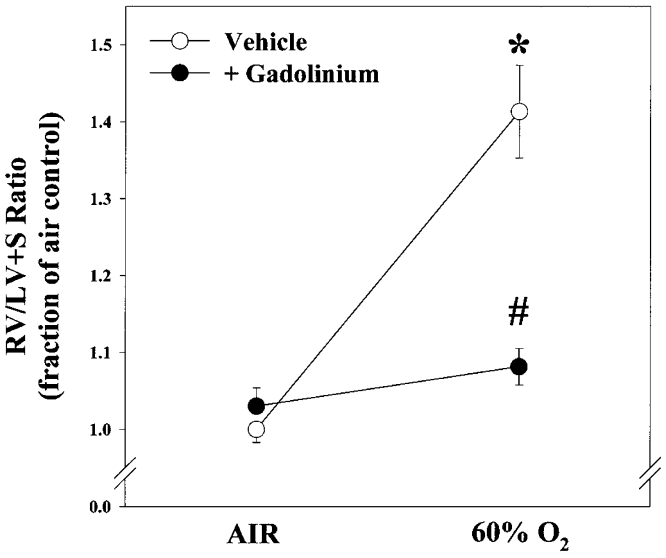


**Figure 3.** RVH. Right ventricular (*RV*) dry weight compared with that of the combined left ventricle and septum (*LV+S*), as an index of RVH, after exposure to air or 60% $O_2$ for 14 d. Newborn rats received i.p. injections on d 0 and d 7 of $GdCl_3$ (10 mg/kg) in 0.9% saline vehicle (*closed circles*) or 0.9% saline vehicle alone (*open circles*). The injection of $GdCl_3$ attenuated the 60% $O_2$-mediated increase in RVH. Plot points represent mean ± SEM for four litters. *$p < 0.05$, by one-way ANOVA, for vehicle-treated animals exposed to 60% $O_2$ compared with those in air. #$p < 0.05$, by one-way ANOVA, for $GdCl_3$-treated animals compared with vehicle-treated animals exposed to 60% $O_2$.

***Institutional review.*** All procedures involving animals were conducted according to criteria established by the Canadian Council for Animal Care. Approval for the study was obtained from the Animal Care Review Committee of the Samuel Lunenfeld Research Institute, Mount Sinai Hospital.

***Exposure system.*** The exposure system has been described in detail previously (21, 23, 24). Briefly, pathogen-free, timed pregnant Sprague Dawley rats (250–275 g) were obtained from Charles River (St. Constant, QC, Canada). Experiments were conducted as paired exposures, with one chamber receiving 60% $O_2$ and the other receiving air. On the anticipated day of delivery, each dam was placed in a 60 × 48 × 25-cm plastic chamber with 12 h/12 h light-dark cycles, with temperature maintained at 25 ± 1°C, minimal humidity, and a $CO_2$ concentration of <0.5%. Equal litter sizes (10–12 pups) were maintained between paired chambers. Food and water were available *ad libitum*. Dams were exchanged daily between chambers to prevent maternal $O_2$ toxicity. At the termination of each exposure period, animals were killed by ether inhalation.

***Interventions.*** Pups were maintained in four paired chambers (air and $O_2$) for a 14-d exposure period. Injections (5 $\mu$L/g body weight) were given i.p. *via* a 30-gauge needle into the right iliac fossa, as previously described for delivery of liposomes, drugs, and antibodies to the lungs of neonatal rats (23, 24, 27, 28). For the intervention with $GdCl_3$, each pair received either 0.9% NaCl (vehicle control) or $GdCl_3.6H_2O$ in 0.9% NaCl (2 mg/mL and 10 mg/kg) within 6 h of birth and on day 7. For the intervention with U74389G, a 21-aminosteroid antioxidant, each pair received either CS-4 (vehicle control) or U74389G in CS-4 (2 mg/mL and 10 mg/kg) within 6 h of birth and daily thereafter as previously described (24). For the intervention with SB217242, a mixed endothelin receptor antagonist (29), each pair received either 0.9% NaCl (vehicle control) or SB217242 (1 mg/mL and 5 mg/kg) within 6 h of birth and daily thereafter.

***Examination of RVH.*** RVH is a well-established index of pulmonary hypertension (30), and has been shown to have a direct correlation with vascular smooth muscle hyperplasia in this model (22). At sacrifice, the thoracic contents were removed *en bloc*. The heart was then separated from the lungs and the right ventricle was dissected free from the left ventricle

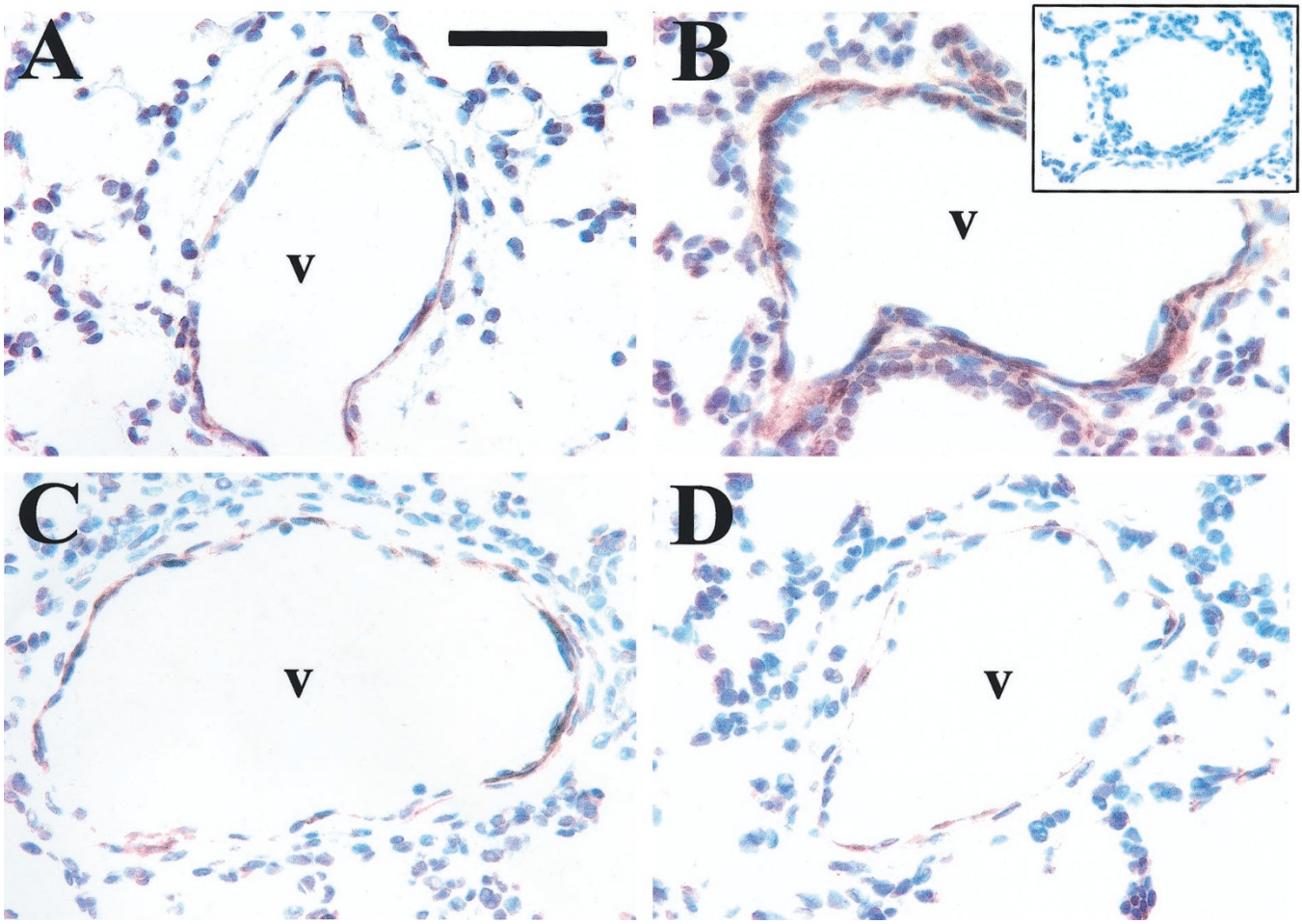


**Figure 4.** Effect of $GdCl_3$ on 60% $O_2$-mediated increased pulmonary vascular smooth muscle mass. Immunohistochemistry for α-smooth muscle actin (*brown stain*) in medium-sized pulmonary vessels (*v*) after exposure to air or 60% $O_2$ for 14 d. Newborn rats received i.p. injections on d 0 and d 7 of $GdCl_3$ (10 mg/kg) in 0.9% saline vehicle or 0.9% saline vehicle alone. Bar length = 250 μm. (*A*) Smooth muscle was evident around vessels of air-exposed pups that received vehicle. (*B*) A large increase in smooth muscle was evident around the vessels of 60% $O_2$-exposed pups that received vehicle. *Inset:* negative control where the primary antiserum was omitted. (*C*) The smooth muscle around vessels in the lungs of air-exposed pups that received $GdCl_3$ did not appear different from air-exposed control animals. (*D*) The lungs of 60% $O_2$-exposed pups that received $GdCl_3$ did not show an increase in perivascular smooth muscle.

with the septum. Each component was freeze-dried and weighed separately.

***Immunohistochemistry.*** Animals were anesthetized with i.p. ketamine (80 mg/kg) and xylazine (20 mg/kg). The pulmonary circulation was flushed with PBS containing 1 U/mL heparin to clear the lungs of blood, and perfusion fixed with 4% (wt/vol) paraformaldehyde while a constant airway pressure of 10 cm $H_2O$ was maintained *via* a tracheal catheter. Before immunohistochemical staining, lung sections were examined to confirm a normal lung structure from air-exposed control pups, and the presence of patchy areas of interstitial thickening and emphysema in 60% $O_2$-exposed pups (21). When lung sections were examined for the presence of macrophages, dilutions of the primary and secondary antisera were 1:100 and 1:250, respectively. Interstitial and alveolar macrophage numbers were quantified by counting of positively stained cells per high-power field (four animals per group and four fields per animal). For α-smooth muscle actin, dilutions of the primary and secondary antisera were 1:1200 and 1:300, respectively. For ET-1, dilutions of the primary and secondary antisera were 1:300 and 1:200, respectively. For the detection of nitrotyrosine residues, dilutions of both primary and secondary antibodies were 1:300. Several methods were used as controls for the specificity of nitrotyrosine immunostaining as described in detail by Viera *et al.* (31). Briefly, these included blocking the primary antiserum with 10 mM nitrotyrosine and reduction of nitrotyrosine *in situ* to aminotyrosine. A positive control for nitrotyrosine immunostaining was generated by addition of 100 mM peroxynitrite to tissue sections. For all other antibodies, antibody specificity was verified by omitting the primary antiserum. After completion of immunohistochemical studies, using an avidin-biotin-peroxidase complex method (32), slides were counterstained with Carazzi hematoxylin, dehydrated, cleared in xylene, and mounted.

***Total (free and esterified) 8-isoprostane measurement.*** To prevent auto-oxidation, lung tissue or cell culture medium was immediately flash frozen with liquid $N_2$ and stored at −80°C until analysis. Upon thawing, 0.005% (wt/vol) butylated hydroxytoluene was added to cell culture medium or tissue homogenized in 1 × PBS. [$^3$H]Prostaglandin $F_{2\alpha}$ (5000 cpm) was added to quantify recovery after purification. Proteins were precipitated by ethanol and removed by centrifugation.

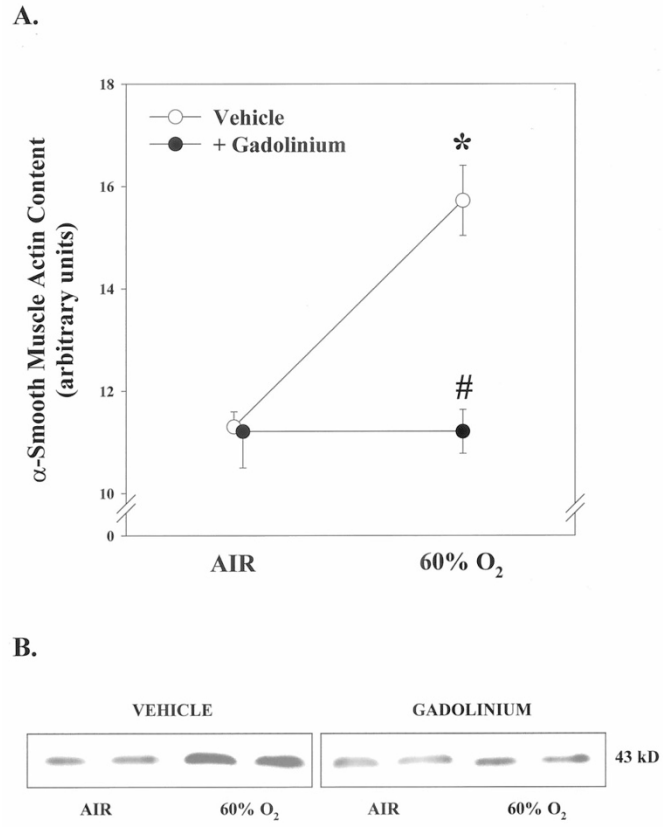


**Figure 5.** Effect of $GdCl_3$ on $\alpha$-smooth muscle actin content of whole lung. (*A*) Lung $\alpha$-smooth muscle actin protein increased after exposure to 60% $O_2$ for 14 d relative to animals exposed to air. Newborn rats received i.p. injections on d 0 and d 7 of $GdCl_3$ (10 mg/kg) in 0.9% saline vehicle (*closed circles*) or 0.9% saline vehicle alone (*open circles*). $GdCl_3$ prevented the 60% $O_2$-mediated increase in $\alpha$-smooth muscle actin. Plot points represent mean ± SEM for 3 litters. $*p < 0.05$, by one-way ANOVA, for animals exposed to 60% $O_2$ compared with those in air in the same treatment group. $\#p < 0.05$, by one-way ANOVA, for $GdCl_3$-treated animals compared with vehicle-treated animals exposed to 60% $O_2$. (*B*) Examples of Western blots for $\alpha$-smooth muscle actin in whole lung after exposure to air or 60% $O_2$ for 14 d. Newborn rats received i.p. injections of either $GdCl_3$ (*GADOLINIUM*) or vehicle alone (*VEHICLE*). Protein size is in kilodaltons.

The supernatant was incubated with an equal volume of 15% (wt/vol) potassium hydroxide at 40°C for a 1-h alkaline hydrolysis of esterified lipid before solid phase extraction using Sep Pak C18 cartridges as previously described (28). After purification, samples were analyzed in duplicate for 8-isoprostane content using a commercially available enzyme immunoassay kit. Recovery from the purification step was analyzed by liquid scintillation counting of the extract and values expressed as picograms per milligram protein for tissue or picograms per milliliter for cell culture medium.

***Lung volume-pressure loops.*** Animals were anesthetized with sodium pentobarbitone (5–10 mg/kg) and paralyzed with pancuronium bromide (0.3 mg/kg). After tracheotomy, the lungs were degassed and volume-pressure loops in the open chest recorded as previously described (21).

***Protein analysis.*** Western blot analysis on lung tissue was performed using protein from lung homogenates. Samples and recombinant protein standards were fractionated by SDS PAGE for 2 h at 120 V. For $\alpha$-smooth muscle actin (43 kD), 20 $\mu$g per lane of protein was fractionated under reducing conditions on 8% to 16% (wt/vol) graded tris-glycine gels and transferred to PVDF membranes. For ET-1 (2.5 kD), 40 $\mu$g per lane of protein was fractionated under nonreducing conditions on 16% (wt/vol) tricine gels and transferred to PVDF membranes. Membranes were blocked with 3% nonfat milk for >1 h, washed in TBS (Tris base 20 mM, NaCl 137 mM, pH 7.6) with 0.1% Tween 20, incubated with appropriate primary antibodies for >1 h followed by further washing and secondary antibody for >1 h. For $\alpha$-smooth muscle actin, dilutions of primary and secondary antibodies were 1:5000 and 1:2800, respectively. For ET-1, dilutions of primary and secondary antibodies were 1:1000 and 1:20,000, respectively. The protein bands were imaged using an enhanced chemiluminescence kit (Amersham Pharmacia Biotech, Piscataway, NJ, U.S.A) and exposed for 30–120 s on Kodak X-Omat Blue XB-1 film (Eastman Kodak, Rochester, NY, U.S.A.). The films were electronically scanned and the band densities were quantified using Scion Image software (Version 1.6, National Institutes of Health, Bethesda, MD, U.S.A.). Equal protein loading was confirmed by Coomassie blue staining of all gels.

***Strain of fetal lung cells in organotypic culture.*** Primary mixed lung cell cultures were prepared from d-19 rat fetuses as previously described (33). Briefly, after removal of the heart, major vessels, and airways, the combined lungs were minced with scissors. The tissue was then subjected to sequential enzymatic dissociation, initially using 1 mg/mL trypsin and 0.01 mg/mL DNase. Disaggregated fetal lung cells reaggregate within Gelfoam sponges to form highly organized alveolar-like structures (34). Cells were cultured on sponges as described previously (35). Briefly, cells were inoculated on $2 \times 2 \times 0.25$-cm Gelfoam sponges at a density of $10 \times 10^6$ cells per sponge and incubated for 72 h in DMEM with 10% (vol/vol) FBS at a gas phase of 21% $O_2$, 5% $CO_2$, and 74% $N_2$ at 37°C. The organotypic cell cultures were then subjected to mechanical strain for comparison with unstrained control cultures. Sponges were placed in DMEM or DMEM with $GdCl_3$ (0.1, 1, or 10 $\mu$M). The mechanical strain device has been described in detail elsewhere (35). Briefly, the unit consisted of a programmable burst timer, a control unit, a regulated DC power supply, and a set of solenoids. A culture dish with a Gelfoam sponge was placed in front of each solenoid. One end of each sponge was fixed to the dish and the other end was attached to a movable metal bar. The movement of the metal bar and sponge was driven by the magnetic force and the recoil property of the sponge. The whole solenoid strain unit was placed in an incubator at a gas phase of 21% $O_2$, 5% $CO_2$, and 74% $N_2$ at 37°C. As previously described for optimal DNA synthesis (35), intermittent strain was at 60 cycles/min with 15-min strain/h and a 5% elongation of the sponge for 24 h.

***Total nitric oxide assay.*** Culture medium in which Gelfoam sponges had been immersed was analyzed for total nitrite ($NO_2^-$) as a quantitative measure of nitric oxide production using a commercially available colorimetric assay. This assay is based on the enzymatic conversion of nitrate [$NO_3^-$ to $NO_2^-$ by nitrate reductase followed by measurement of $NO_2^-$ by the Griess reaction (36)]. The detection limit of the assay is ≥1.35 nmol/mL.

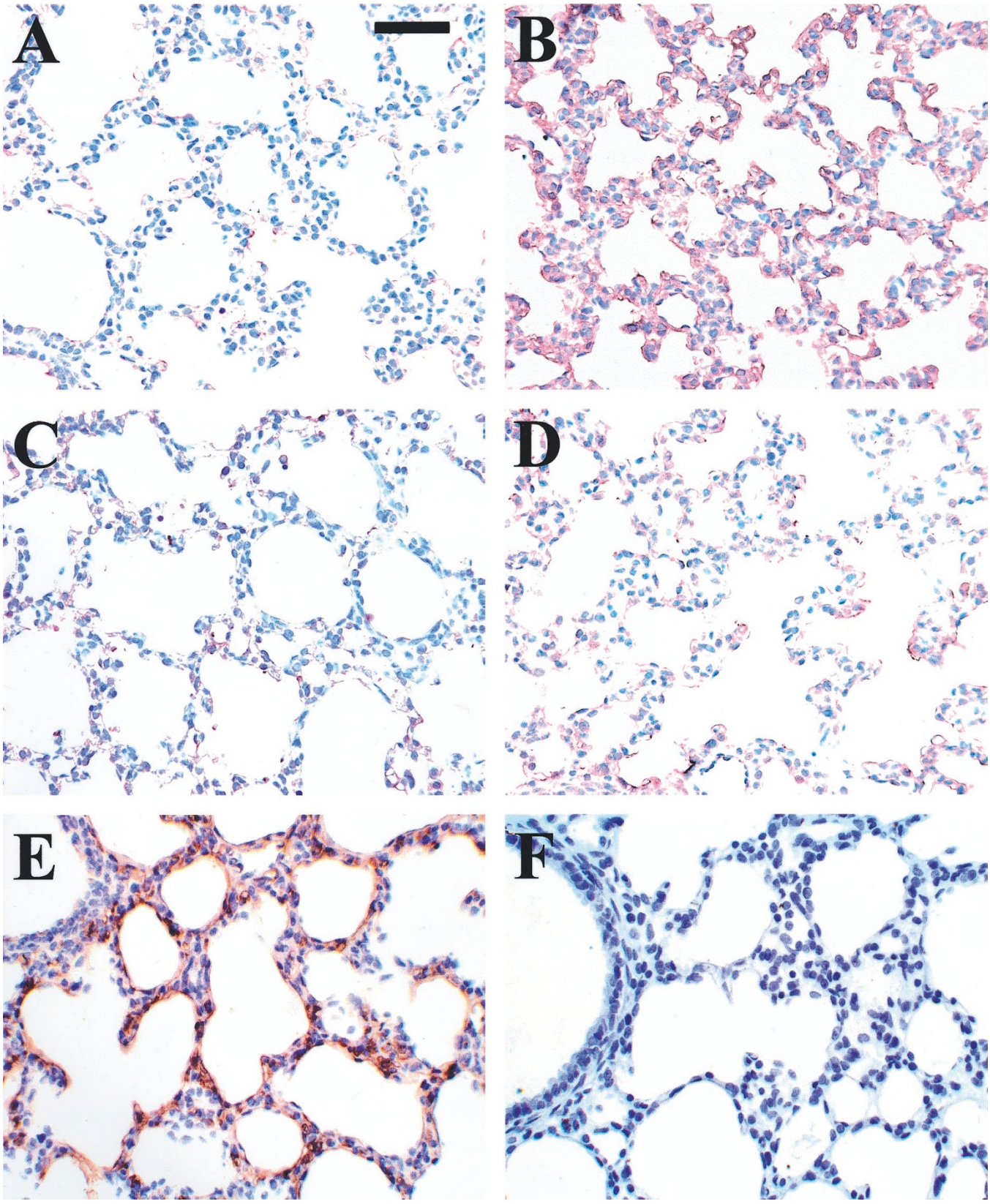


**Figure 6.** Immunohistochemistry for nitrotyrosine (*brown stain*), a marker of protein nitration, in lung tissue after exposure to air or 60% $O_2$ for 7 d. On the day of birth, rat pups received a single i.p. injection of $GdCl_3$ (10 mg/kg) in 0.9% saline or 0.9% saline alone. Bar length = 250 $\mu$m. (*A*) Air-exposed pups that received vehicle had negligible nitrotyrosine staining. (*B*) The 60% $O_2$-exposed pups that received vehicle had abundant nitrotyrosine formation. (*C*) Lung tissue from air-exposed pups that received $GdCl_3$ had a similar appearance to air-exposed control pups. (*D*) The 60% $O_2$-exposed pups that received $GdCl_3$ had a marked reduction in nitrotyrosine staining. (*E*) Positive control staining produced by the addition of 100 mM peroxynitrite. (*F*) Negative control staining in which the primary antiserum was blocked with 10 mM nitrotyrosine.

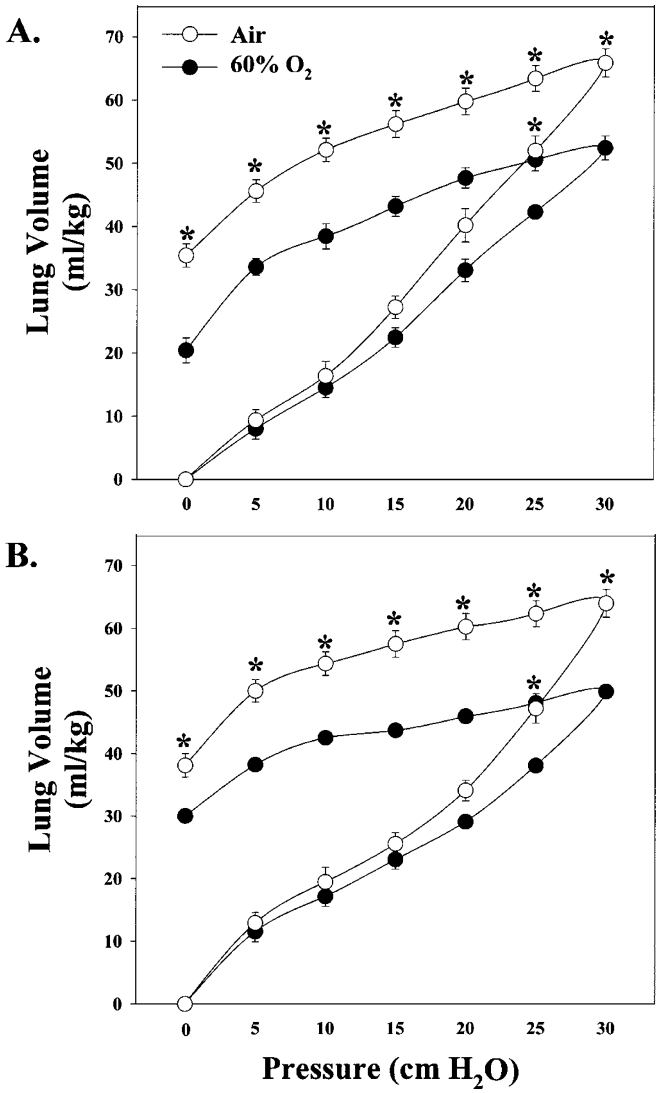


**Figure 7.** Lung mechanics. The effect of air (*open circles*) or 60% $O_2$ (*closed circles*) on lung volume-pressure loops at d 14 in newborn rats that received 0.9% NaCl vehicle (*A*) or $GdCl_3$ (10 mg/kg) in 0.9% NaCl vehicle (*B*) on d 0 and d 7 by i.p. injection. Plot points represent mean ± SEM for four or five pups. *$p < 0.05$, by one-way ANOVA, for $O_2$-exposed animals compared with air controls for the same pressure.

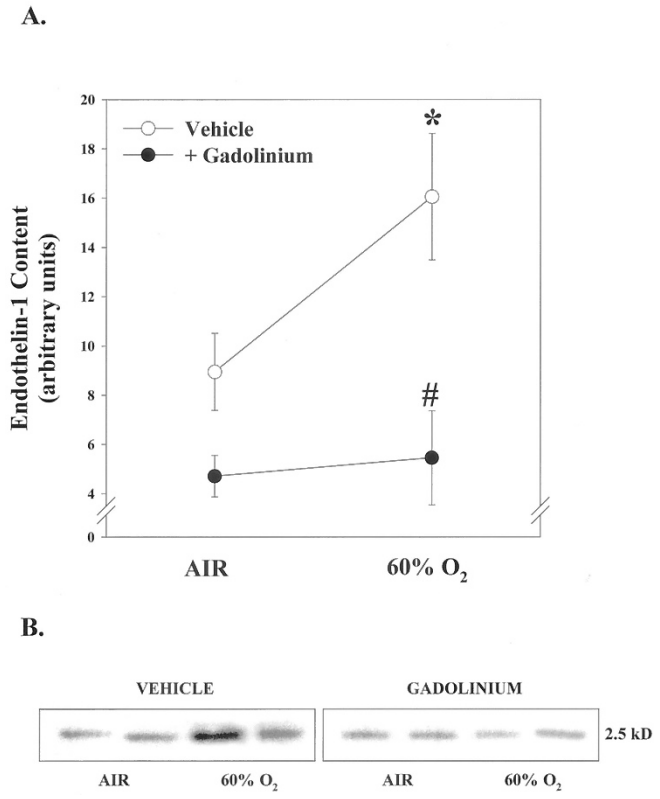


**Figure 8.** Effect of $GdCl_3$ on ET-1 content in whole lung. (*A*) ET-1 expression increased after exposure to 60% $O_2$ for 14 d relative to values for air-exposed animals. Newborn rats received i.p. injections on d 0 and d 7 of $GdCl_3$ (10 mg/kg) in 0.9% saline vehicle (*closed circles*) or 0.9% saline vehicle alone (*open circles*). Treatment with $GdCl_3$ attenuated the 60% $O_2$-dependent increase in ET-1 expression. Plot points represent mean ± SEM for three litters. *$p < 0.05$, by one-way ANOVA, for animals exposed to 60% $O_2$ compared with those in air in the same treatment group. #$p < 0.05$, by one-way ANOVA, for $GdCl_3$-treated animals compared with vehicle-treated animals exposed to 60% $O_2$. (*B*) Example of Western blot analysis for ET-1 in whole lung after exposure to air or 60% $O_2$ for 14 d. Newborn rats received i.p. injections of either $GdCl_3$ (*GADOLINIUM*) or vehicle alone (*VEHICLE*). Protein size is in kilodaltons.

***ET-1 measurement.*** Unpurified culture medium was analyzed for ET-1 content using a commercially available enzyme immunoassay kit with a detection limit of ≥32 pg/mL.

***Data presentation.*** Unless otherwise stated, all values are for the mean ± SEM of four litters. Statistical significance ($p < 0.05$) was determined by ANOVA followed by assessment of differences using Duncan's multiple range test (37). Error bars are not evident in figures where they fall within the plot point.

## RESULTS

Immunohistochemical staining of lung sections for macrophage TPRM-2 antigen are shown in Figures 1 and 2. Compared with air controls (Fig. 1*A*), pulmonary accumulation of macrophages was increased after 60% $O_2$ exposure for 14 d (Fig. 1*B*). Air-exposed animals treated with the 21-aminosteroid, U74389G (Fig. 1*C*), had similar macrophage content to vehicle-treated controls. This 60% $O_2$-mediated increase was completely abrogated by treatment with U74389G (Fig. 1*D*).

As shown in Figure 2, compared with air controls at 7 d (Fig. 2*A*), pulmonary accumulation of macrophages was markedly increased (29.25 ± 0.5 macrophages per high-power field *versus* 10.25 ± 2 in air-exposed vehicle-treated animals; $p < 0.05$) after exposure to 60% $O_2$ for 7 d (Fig. 2*B*). Treatment with $GdCl_3$ (Fig. 2, *C* and *D*) markedly reduced the macrophage content of $O_2$-exposed lungs (Fig. 2*D*; 10.75 ± 1.2 macrophages per high-power field *versus* 29.25 ± 0.5 in vehicle-treated animals; $p < 0.05$) to levels comparable to air controls (Fig. 2*A*), in keeping with the known inhibitory effect of $GdCl_3$ on macrophage chemotaxis and survival. In contrast to air-exposed animals at 7 d (Fig. 2*A*), pulmonary macrophages were not evident on the day of birth (Fig. 2*E*). A negative control in which the primary antibody was omitted is shown in Figure 2*F*.

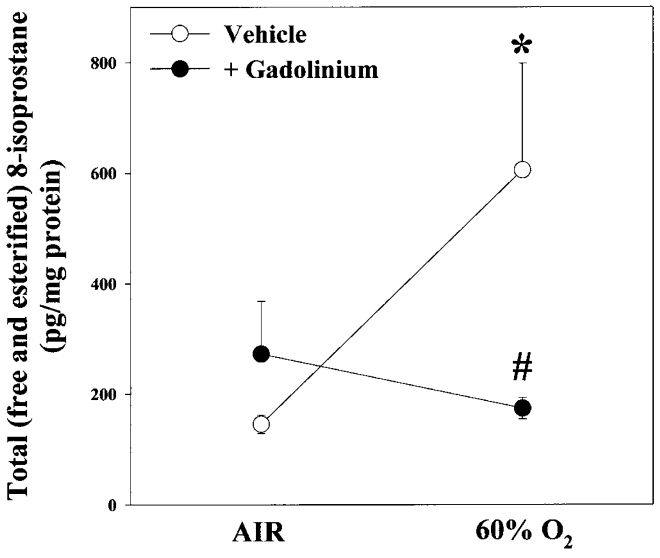


**Figure 9.** Effect of $GdCl_3$ on total (free and esterified) 8-isoprostane in whole lung after exposure to air or 60% $O_2$ for 14 d. Newborn rats received i.p. injections on d 0 and d 7 of $GdCl_3$ (10 mg/kg) in 0.9% saline vehicle (*closed circles*) or 0.9% saline vehicle alone (*open circles*). Treatment with $GdCl_3$ attenuated the 60% $O_2$-dependent increase in 8-isoprostane. Plot points represent mean ± SEM for four litters. *$p < 0.05$, by one-way ANOVA, for animals exposed to 60% $O_2$ compared with those in air in the same treatment group. #$p < 0.05$, by one-way ANOVA, for $GdCl_3$-treated animals compared with vehicle-treated animals exposed to 60% $O_2$.

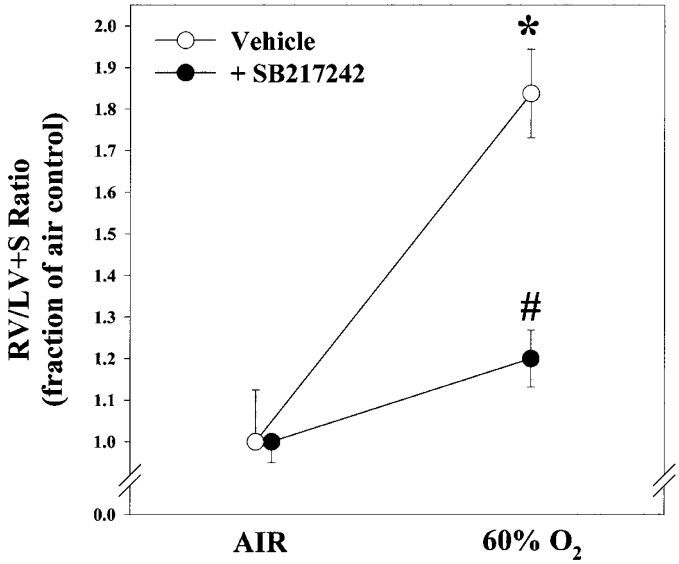


**Figure 10.** Effect of the mixed endothelin receptor antagonist, SB217242, on 60% $O_2$-mediated RVH. Right ventricular (*RV*) dry weight compared with that of the combined left ventricle and septum (*LV+S*), as an index of RVH, after exposure to air or 60% $O_2$ for 14 d. Newborn rats received daily i.p. injections of SB217242 (5 mg/kg) in 0.9% saline vehicle (*closed circles*) or 0.9% saline vehicle alone (*open circles*). The injection of SB217242 attenuated the 60% $O_2$-mediated increase in RVH. Plot points represent mean ± SEM for four litters. *$p < 0.05$, by one-way ANOVA, for vehicle-treated animals exposed to 60% $O_2$ compared with those in air. #$p < 0.05$, by one-way ANOVA, for SB217242-treated animals compared with vehicle-treated animals exposed to 60% $O_2$.

Vehicle-treated 60% $O_2$-exposed animals had significant RVH ($p < 0.05$), as assessed by the ratio of the right ventricle to the left ventricle and septum dry weights, compared with both vehicle- and $GdCl_3$-treated air-exposed control animals (Fig. 3). This 60% $O_2$-induced RVH, an index of pulmonary hypertension, was completely attenuated ($p < 0.05$) in animals treated with $GdCl_3$. Smooth muscle mass was assessed by $\alpha$-smooth muscle actin immunohistochemistry (Fig. 4) and Western blot analysis (Fig. 5). Compared with air-exposed controls (Fig. 4*A*), vehicle-treated 60% $O_2$-exposed animals showed a marked increase in immunoreactive arterial smooth muscle (Fig. 4*B*), and an increase in total lung $\alpha$-smooth muscle actin content (Fig. 5; $p < 0.05$). Animals treated with $GdCl_3$ (Fig. 4, *C* and *D*) did not have evidence of these $O_2$-induced smooth muscle changes (Fig. 4*D* and Fig. 5; $p < 0.05$).

Nitrotyrosine formation in lung tissue, a marker of protein nitration by reactive nitrogen species such as peroxynitrite, was assessed by immunohistochemistry (Fig. 6). When compared with air-exposed controls (Fig. 6*A*), vehicle-treated animals exposed to 60% $O_2$ for 7 d (Fig. 6*B*) showed abundant nitrotyrosine formation. Treatment with $GdCl_3$ (Fig. 6, *C* and *D*) prevented this $O_2$-mediated increase in nitrotyrosine (Fig. 6*D*). Positive (addition of 100 mM peroxynitrite; Fig. 6*E*) and negative (omission of primary antibody; Fig. 6*F*) controls are shown.

As previously described (21), the lungs of rat pups exposed to 60% $O_2$ for 14 d have areas of apparent emphysema interspersed with patchy areas of parenchymal thickening and, consistent with these changes, abnormal lung mechanics. When compared with these previously reported changes (21), we could not detect any obvious effect of treatment with $GdCl_3$ on either macroscopic structural changes (data not shown) or on lung volume-pressure loops (Fig. 7, *A* and *B*).

The effect of treatment with $GdCl_3$ on possible mediators of $O_2$-induced pulmonary hypertension was also examined. ET-1 expression was studied by Western blot analysis (Fig. 8), whereas 8-isoprostane (Fig. 9) was quantified by enzyme immunoassay. Exposure of vehicle-treated animals to 60% $O_2$ for 14 d led to an increase in ET-1 in lung tissue (Fig. 8). This 60% $O_2$-mediated increase in ET-1 was prevented ($p < 0.05$) by treatment with $GdCl_3$ (Fig. 8). There seemed to be a small effect of treatment with $GdCl_3$ on ET-1 expression in the lung tissue of air-exposed control animals, but this was not statistically significant ($p > 0.05$). Similarly, the 60% $O_2$-mediated increase in lung 8-isoprostane content was completely attenuated ($p < 0.05$) by $GdCl_3$ (Fig. 9).

Because any effects of $GdCl_3$ could be mediated through inhibition of stretch-activated cation channels, in addition to inhibition of macrophage accumulation and activation, we examined the effect of $GdCl_3$ on organotypic cultures of rat fetal lung cells exposed to mechanical strain. After 24 h of mechanical strain, ET-1 was significantly ($p < 0.05$) increased in cell culture medium (660 ± 93 pg/mL *versus* 303 ± 58 pg/mL in unstrained control cultures; $n = 4$). $GdCl_3$ (0.1–10 $\mu$M) had no effect ($p > 0.05$) on this stretch-mediated increase. Mechanical strain also had no effect ($p > 0.05$) on 8-isoprostane or nitrite content in cell culture medium (data not shown).

Neonatal pups treated with a mixed ET-1 receptor antagonist, SB217242, did not develop 60% $O_2$-mediated RVH (Fig. 10).

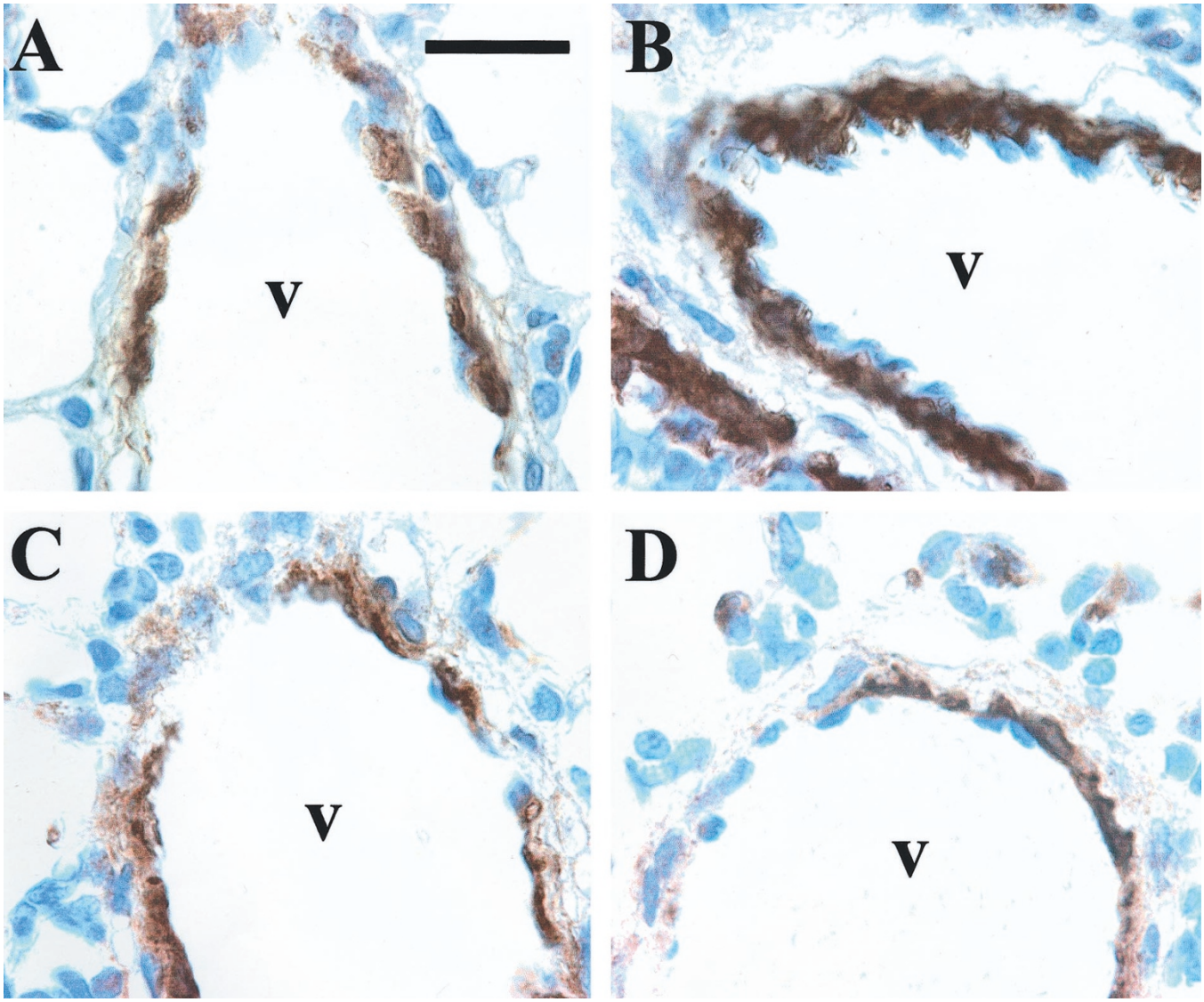


**Figure 11.** Effect of SB217242 on 60% $O_2$-mediated increased pulmonary vascular smooth muscle mass. Immunohistochemistry for $\alpha$-smooth muscle actin (*brown stain*) in medium-sized pulmonary vessels (*v*) after exposure to air or 60% $O_2$ for 14 d. Newborn rats received daily i.p. injections of SB217242 (5 mg/kg) in 0.9% saline vehicle or 0.9% saline vehicle alone. Bar length = 100 $\mu$m. (*A*) Smooth muscle was evident around vessels of air-exposed pups that received vehicle. (*B*) A large increase in smooth muscle was evident around the vessels of 60% $O_2$-exposed pups that received vehicle. (*C*) The smooth muscle around vessels in the lungs of air-exposed pups that received SB217242 did not appear different from air-exposed control animals. (*D*) The lungs of 60% $O_2$-exposed pups that received SB217242 did not show an increase in perivascular smooth muscle.

Perivascular smooth muscle was assessed by $\alpha$-smooth muscle actin immunohistochemistry (Fig. 11). Compared with vehicle-treated air-exposed controls (Fig. 11*A*), 60% $O_2$-exposed vehicle-treated animals had a marked increase in perivascular smooth muscle mass (Fig. 11*B*). Treatment with SB217242 (Fig. 11, *C* and *D*) prevented this $O_2$-mediated increase in smooth muscle mass (Fig. 11*D*). SB217242 had no impact on 60% $O_2$-mediated lung structural changes (data not shown). These findings confirm that the increase in ET-1 observed with exposure to 60% $O_2$ was causally related to the development of pulmonary hypertension.

## DISCUSSION

Macrophages are differentiated mononuclear phagocytes that may reside in tissues for several months. They are essential for tissue remodeling and wound healing, and congregate during subacute or chronic inflammation. In human preterm infants with respiratory distress, pulmonary macrophage numbers increase early in the second week of life (17), remain elevated in infants who later develop clinical and radiologic features of BPD, and decline in those who recover (18). In adult animals, pulmonary macrophages are present in exaggerated numbers in pulmonary hypertension induced by hypobaric hypoxia (38). Pulmonary macrophages are central to the pathogenesis of pulmonary hypertension induced by monocrotaline injection in rats (39–41) and in antiplatelet serum-induced pulmonary hypertension in sheep (42). As described above, we found pulmonary interstitial macrophages to be greatly increased after exposure to 60% $O_2$. Inhibition of this increase in lung macrophage content and secondary up-regulation of ET-1 prevented RVH and the concomitant increase in smooth mus-

cle cell mass but not other morphologic aspects of lung tissue injury or abnormal lung mechanics.

Abnormalities in vascular tone and smooth muscle mass underlie the pathophysiology of pulmonary hypertension in BPD, although the cellular mechanisms are not fully understood. The pathogenesis of BPD is clearly multifactorial, but it is widely believed that oxidant injury plays a critical role (12). ROS can be generated from multiple sources during hyperoxia. Intracellular production is greatly increased (43, 44), and extracellular formation may be induced by activation of polymorphonuclear leukocytes and macrophages (13, 15). These cells produce other mediators implicated in lung injury, such as ET-1 (14), 8-isoprostane (24), and various growth factors (13).

$GdCl_3$ abrogates macrophage accumulation by induction of apoptosis after phagocytosis (45), but has little effect on polymorphonuclear leukocytes. We found that a commonly used dose of $GdCl_3$ abrogated 60% $O_2$-induced macrophage accumulation in newborn rats. $GdCl_3$ also inhibited $O_2$-mediated nitrotyrosine formation in the lung. Another known effect of $GdCl_3$ is the blockade of stretch-mediated (mechanogated) cation channels, which are involved in cell proliferation and altered gene expression (46). We attempted to elucidate the mechanism of $GdCl_3$ action in our *in vivo* model by subjecting fetal cells in organotypic culture to mechanical strain. We have previously demonstrated that 10 $\mu$M $GdCl_3$ inhibits strain-induced DNA synthesis in this *in vitro* model (47). Our findings *in vitro* suggest that the observed effects of $GdCl_3$ *in vivo* were the result of inhibition of lung macrophage content rather than a blockade of mechanogated ion channels.

Cytokines, many of which are produced by macrophages, act as modulators of cell proliferation in many diseases that share common pathogenic elements. Pulmonary pathologies that are likely to be mediated by abnormal cytokine expression include pulmonary hypertension and pulmonary fibrosis, both of which are components of BPD. As described above, we found that ET-1 and 8-isoprostane are increased during $O_2$ exposure and are abrogated by inhibition of macrophage accumulation. This indicates that macrophages are directly or indirectly involved in the up-regulation of these factors. ET-1 and 8-isoprostane elicit a number of biologic effects in the lung, including smooth muscle cell contraction and proliferation (48, 49) and fibroblast chemotaxis and proliferation (50). Macrophages can synthesize ET-1 (14), or be primed by ET-1 to produce increased quantities of ROS (51). Moreover, the production of ET-1 may be greatly augmented by 8-isoprostane in the lung (24) and other organs (49, 52). Our previous studies (24) demonstrated a 60% $O_2$-mediated, and 8-isoprostane-induced, up-regulation of ET-1 in association with the development of pulmonary hypertension. As described herein, a causal relationship between increased ET-1 expression and the development of pulmonary hypertension has been confirmed by the use of a mixed endothelin ($ET_A/ET_B$) receptor antagonist. Whether macrophages are the primary source of the ET-1 and 8-isoprostane generated during $O_2$ exposure, or whether a macrophage product enhances their formation by another cell type, requires further elucidation. Whatever the source of ET-1 and 8-isoprostane, it is clear that their enhanced production, and the resultant pulmonary hypertension, after exposure to 60% $O_2$ are macrophage dependent.

Taken together, the findings reported above suggest that pulmonary macrophages are important in the pathogenesis of $O_2$-mediated pulmonary hypertension. The findings that $GdCl_3$ did not alter either abnormal lung morphology or lung mechanics induced by 60% $O_2$ indicate that reactive nitrogen species, 8-isoprostane, and ET-1 may not be involved in these aspects of $O_2$-induced lung injury. These findings are consistent with our previously reported observations with an antioxidant intervention (24), in that different components of $O_2$-induced lung injury seem to be regulated by different mediators and cell types.

## REFERENCES


1. Edwards DK, Dyer WM, Northway WH 1977 Twelve years' experience with bronchopulmonary dysplasia. Pediatrics 59:839–846
2. O'Brodovich HM, Mellins RB 1985 Bronchopulmonary dysplasia. Unresolved acute neonatal lung injury. Am Rev Respir Dis 132:694–709
3. Jacob SV, Coates AL, Lands LC, MacNeish CF, Riley SP, Hornby L, Outerbridge EW, Davis GM, Williams RL 1998 Long-term pulmonary sequelae of severe bronchopulmonary dysplasia. J Pediatr 133:193–200
4. Coalson JJ 2000 Pathology of chronic lung disease of early infancy. In: Bland RD, Coalson JJ (eds) Chronic Lung Disease in Early Infancy. Marcel Dekker, New York, pp 85–124
5. Subhedar NV, Hamdan AH, Ryan SW, Shaw NJ 1998 Pulmonary artery pressure: early predictor of chronic lung disease in preterm infants. Arch Dis Child Fetal Neonatal Ed 78:F20–F24
6. Bush A, Busst CM, Knight WB, Hislop AA, Haworth SG, Shinebourne EA 1990 Changes in pulmonary circulation in severe bronchopulmonary dysplasia. Arch Dis Child 65:739–745
7. Goodman G, Perkin RM, Anas NG, Sperling DR, Hicks DA, Rowen M 1988 Pulmonary hypertension in infants with bronchopulmonary dysplasia. J Pediatr 112:67–72
8. Fitzgerald D, Evans N, Van Asperen P, Henderson-Smart D 1994 Subclinical persisting pulmonary hypertension in chronic neonatal lung disease. Arch Dis Child Fetal Neonatal Ed 70:F118–F122
9. Gill AB, Weindling AM 1995 Raised pulmonary artery pressure in very low birth weight infants requiring supplemental oxygen at 36 weeks after conception. Arch Dis Child Fetal Neonatal Ed 72:F20–F22
10. Tomashefski Jr JF, Oppermann HC, Vawter GF, Reid LM 1984 Bronchopulmonary dysplasia: a morphometric study with emphasis on the pulmonary vasculature. Pediatr Pathol 2:469–487
11. Stocker JT 1986 Pathologic features of long-standing "healed" bronchopulmonary dysplasia: a study of 28 3- to 40-month-old infants. Hum Pathol 17:943–961
12. Saugstad OD 1997 Bronchopulmonary dysplasia and oxidative stress: are we closer to an understanding of the pathogenesis of BPD? Acta Paediatr 86:1277–1282
13. Nathan CF 1987 Secretory products of macrophages. J Clin Invest 79:319–326
14. Ehrenreich H, Anderson RW, Fox CH, Rieckmann P, Hoffman GS, Travis WD, Coligan JE, Kehrl JH, Fauci AS 1990 Endothelins, peptides with potent vasoactive properties, are produced by human macrophages. J Exp Med 172:1741–1748
15. Speer CP 1999 Inflammatory mechanisms in neonatal chronic lung disease. Eur J Pediatr 158:S18–S22
16. Jacobs RF, Wilson CB, Palmer S, Springmeyer SC, Henderson WR, Glover DM, Kessler Jr DL, Murphy JH, Hughes JP, van Belle G, Chi EY, Hodson WA 1985 Factors related to the appearance of alveolar macrophages in the developing lung. Am Rev Respir Dis 131:548–553
17. Merritt TA, Stuard ID, Puccia J, Wood B, Edwards DK, Finkelstein J, Shapiro DL 1981 Newborn tracheal aspirate cytology: classification during respiratory distress syndrome and bronchopulmonary dysplasia. J Pediatr 98:949–956
18. Clement A, Chadelat K, Sardet A, Grimfield A, Tournier G 1988 Alveolar macrophage status in bronchopulmonary dysplasia. Pediatr Res 23:470–473
19. Meyrick B, Reid L 1982 Pulmonary arterial and alveolar development in normal postnatal rat lung. Am Rev Respir Dis 125:468–473
20. Hislop A, Reid L 1978 Normal structure and dimensions of the pulmonary arteries in the rat. J Anat 125:71–83
21. Han RN, Buch S, Tseu I, Young J, Christie NA, Frndova H, Lye SJ, Post M, Tanswell AK 1996 Changes in structure, mechanics, and insulin-like growth factor-related gene expression in the lungs of newborn rats exposed to air or 60% oxygen. Pediatr Res 39:921–929
22. Koppel R, Han RN, Cox D, Tanswell AK, Rabinovitch M 1994 Alpha 1-antitrypsin protects neonatal rats from pulmonary vascular and parenchymal effects of oxygen toxicity. Pediatr Res 36:763–770
23. Buch S, Han RNN, Cabacungan J, Wang J, Yuan S, Belcastro R, Deimling J, Luo X, Lye SJ, Post M, Tanswell AK 2000 Changes in expression of platelet-derived growth factor and its receptors in the lungs of newborn rats exposed to air or 60% $O_2$. Pediatr Res 48:423–433

24. Jankov RP, Luo X, Cabacungan J, Belcastro R, Frndova H, Lye SJ, Tanswell AK 2000 Endothelin-1 and $O_2$-mediated pulmonary hypertension in neonatal rats: a role for products of lipid peroxidation. Pediatr Res 48:289–298
25. Pendino KJ, Meidhof TM, Heck DE, Laskin JD, Laskin DL 1995 Inhibition of macrophages with gadolinium chloride abrogates ozone-induced pulmonary injury and inflammatory mediator production. Am J Respir Cell Mol Biol 13:125–132
26. Singh B, de la Concha-Bermejillo A 1998 Gadolinium chloride removes pulmonary intravascular macrophages and curtails the degree of ovine lentivirus-induced lymphoid interstitial pneumonia. Int J Exp Pathol 79:151–162
27. Tanswell AK, Freeman BA 1987 Liposome-entrapped antioxidant enzymes prevent lethal $O_2$ toxicity in the newborn rat. J Appl Physiol 63:347–352
28. Luo X, Sedlackova L, Belcastro R, Cabacungan J, Lye SJ, Tanswell AK 1999 Effect of the 21-aminosteroid U74389G on oxygen-induced free radical production, lipid peroxidation, and inhibition of lung growth in neonatal rats. Pediatr Res 46:215–223
29. Ohlstein EH, Nambi P, Lago A, Hay DW, Beck G, Fong KL, Eddy EP, Smith P, Ellens H, Elliott JD 1996 Nonpeptide endothelin receptor antagonists. VI: Pharmacological characterization of SB 217242, a potent and highly bioavailable endothelin receptor antagonist. J Pharmacol Exp Ther 276:609–615
30. Fulton RM, Hutchinson EC 1952 Ventricular weight in cardiac hypertrophy. Br Heart J 14:413–420
31. Viera L, Ye YZ, Estevez AG, Beckman JS 1999 Immunohistochemical methods to detect nitrotyrosine. Methods Enzymol 301:373–381
32. Hsu SM, Raine L, Fanger H 1981 Use of avidin-biotin-peroxidase complex (ABC) in immunoperoxidase techniques: a comparison between ABC and unlabeled antibody (PAP) procedures. J Histochem Cytochem 29:577–580
33. Tanswell AK, Tzaki MG, Byrne PJ 1986 Hormonal and local factors influence antioxidant enzyme activity of rat fetal lung cells *in vitro*. Exp Lung Res 11:49–59
34. Simpson LL, Tanswell AK, Joneja MG 1985 Epithelial cell differentiation in organotypic cultures of fetal rat lung. Am J Anat 172:31–40
35. Liu M, Skinner SJ, Xu J, Han RN, Tanswell AK, Post M 1992 Stimulation of fetal rat lung cell proliferation *in vitro* by mechanical stretch. Am J Physiol 263:L376–L383
36. Miles AM, Wink DA, Cook JC, Grisham MB 1996 Determination of nitric oxide using fluorescence spectroscopy. Methods Enzymol 268:105–120
37. Snedecor GW, Cochran WG 1980 Statistical Methods. Iowa State University Press, Ames, Iowa, pp 215–295
38. Sulkowska M 1997 Morphological studies of the lungs in chronic hypobaric hypoxia. Pol J Pathol 48:225–234
39. Sugita T, Stenmark KR, Wagner Jr WW, Henson PM, Henson JE, Hyers TM, Reeves JT 1983 Abnormal alveolar cells in monocrotaline induced pulmonary hypertension. Exp Lung Res 5:201–215
40. Miyata M, Sakuma F, Yoshimura A, Ishikawa H, Nishimaki T, Kasukawa R 1995 Pulmonary hypertension in rats. Role of bromodeoxyuridine-positive mononuclear cells and alveolar macrophages. Int Arch Allergy Immunol 108:281–286
41. Kimura H, Kasahara Y, Kurosu K, Sugito K, Takiguchi Y, Terai M, Mikata A, Natsume M, Mukaida N, Matsushima K, Kuriyama T 1998 Alleviation of monocrotaline-induced pulmonary hypertension by antibodies to monocyte chemotactic and activating factor/monocyte chemoattractant protein-1. Lab Invest 78:571–581
42. Nakano T, Miyamoto K, Nishimura M, Aida A, Aoi K, Kawakami Y 1994 Role of pulmonary intravascular macrophages in anti-platelet serum-induced pulmonary hypertension in sheep. Respir Physiol 98:83–99
43. Freeman BA, Crapo JD 1981 Hyperoxia increases oxygen radical production in rat lungs and lung mitochondria. J Biol Chem 256:10986–10992
44. Freeman BA, Topolosky MK, Crapo JD 1982 Hyperoxia increases oxygen radical production in rat lung homogenates. Arch Biochem Biophys 216:477–484
45. Mizgerd JP, Molina RM, Stearns RC, Brain JD, Warner AE 1996 Gadolinium induces macrophage apoptosis. J Leukoc Biol 59:189–195
46. Caldwell RA, Clemo HF, Baumgarten CM 1998 Using gadolinium to identify stretch-activated channels: technical considerations. Am J Physiol 275:C619–C621
47. Liu M, Xu J, Tanswell AK, Post M 1994 Inhibition of mechanical strain-induced fetal rat lung cell proliferation by gadolinium, a stretch activated channel blocker. J Cell Physiol 161:501–507
48. Zamora MR, Stelzner TJ, Webb S, Panos RJ, Ruff LJ, Dempsey EC 1996 Overexpression of endothelin-1 and enhanced growth of pulmonary artery smooth muscle cells from fawn-hooded rats. Am J Physiol 270:L101–L109
49. Lahaie I, Hardy P, Hou X, Hassessian H, Asselin P, Lachapelle P, Almazan G, Varma DR, Morrow JD, Roberts II LJ, Chemtob S 1998 A novel mechanism for vasoconstrictor action of 8-isoprostaglandin F2 alpha on retinal vessels. Am J Physiol 274:R1406–R1416
50. Peacock AJ, Dawes KE, Shock A, Gray AJ, Reeves JT, Laurent GJ 1992 Endothelin-1 and endothelin-3 induce chemotaxis and replication of pulmonary artery fibroblasts. Am J Respir Cell Mol Biol 7:492–499
51. Kojima T, Hattori K, Hirata Y, Aoki T, Sasai-Takedatsu M, Kino M, Kobayashi Y 1996 Endothelin-1 has a priming effect on production of superoxide anion by alveolar macrophages: its possible correlation with bronchopulmonary dysplasia. Pediatr Res 39:112–116
52. Takahashi K, Nammour TM, Fukunaga M, Ebert J, Morrow JD, Roberts LJD, Hoover RL, Badr KF 1992 Glomerular actions of a free radical-generated novel prostaglandin, 8-epi-prostaglandin F2 alpha, in the rat. Evidence for interaction with thromboxane A2 receptors. J Clin Invest 90:136–141